Retention Behavior of Star-Shaped Polystyrene near the Chromatographic Critical Condition

Kyuhyun Im, Hae-Woong Park, Youngtak Kim, Sunyoung Ahn, and Taihyun Chang*

Department of Chemistry and Polymer Research Institute, Pohang University of Science and Technology, Pohang 790-784, Korea

Kwanyoung Lee and Hyung-Jae Lee

Kumho Petrochemical Co., Ltd., R&D Center, P.O. Box 64, Yuseong, Daejeon 305-600, Korea

Jesse Ziebarth and Yongmei Wang*

Department of Chemistry, The University of Memphis, Memphis, Tennessee 38152

Received October 26, 2007; Revised Manuscript Received February 28, 2008

ABSTRACT: The retention behavior of star-shaped polystyrene (PS) at the liquid chromatographic critical condition of linear PS was investigated. The star-shaped PS samples were prepared by anionic polymerization of styrene and subsequent linking of the polystyryl anions with divinylbenzene. The linking reaction yields a series of star-shaped PS with different number of branches of equal length. Three star-shaped PS samples with different arm molecular weight (MW) were prepared. To investigate the MW (hence the branch number) dependence of the LCCC (liquid chromatography at the critical condition) retention, the two-dimensional liquid chromatography method was used—first separating the polymers with respect to the molecular weight and subsequently separating the effluent by LCCC. Two different pore size columns were used for the LCCC separation to investigate the pore size dependence. The LCCC retention shows a very complex behavior. The retention time of the star-shaped PS shows a strong variation with MW (branch number) at the coelution condition of linear PS, and the deviation from the coelution behavior is more serious at a smaller pore sized column. The peculiar LCCC retention behavior was successfully delineated by a lattice Monte Carlo method taking into account the excluded volume and weak attractive interaction of the chain ends.

Introduction

Branched polymers are encountered frequently in commercial polymers such as polyolefin and in natural polymers like polysaccharides. Long chain branching has a significant impact on the rheological and mechanical properties in polymers and can be a valuable attribute in controlling processability and performance.[1,2] In consequence, the rigorous characterization of branched polymers is of importance not only for quality control of the polymeric materials but also for understanding of the relationship between the molecular characteristics and the bulk property.

The characterization of branched polymers is more complicated than linear homopolymers because they have distributions not only in molecular weight (MW) but also in branch number. For the characterization of long chain branching, size exclusion chromatography (SEC) separation coupled with a mass sensitive detector (e.g., light scattering detector) and a chain size sensitive detector (e.g., viscosity detector) has been commonly employed.[3] The measurement of MW (by light scattering detection) and chain size (by viscosity detection) of each fraction is supposed to provide information on the bivariate distribution of MW and branching. The method is based on the assumption that SEC separates the polymers into homogeneous fractions in MW and branching. However, SEC separates polymer according to the hydrodynamic volume and does not yield homogeneous fractions in MW and branching. The heterogeneity of the fractions remains as a potential source of error.

In recent years, non-SEC techniques such as interaction chromatography (IC) and liquid chromatography at the critical condition (LCCC) have made noticeable progress as polymer characterization methods.[4–6] Concerning the characterization of branched polymers, the sensitiveness of IC to MW rather than the chain size allows a far better separation of branched polymers according to the branch number if MW depends on number of branches as in the case of star-shaped polymers with a well-defined MW of branch chains.[7–13] Another successful example of a separation of branched polymers using non-SEC methods is the LCCC separation according to the functionality if a branched polymer contains functional groups which are proportional to the number of branches.[11,14–16] In particular, Im et al. successfully separated star-shaped polymers having broad distribution in both branch MW and branch number by two-dimensional liquid chromatography (2D-LC); the first dimension was TGIC separating the polymer according to their molar mass, and the second dimension was LCCC separating the TGIC effluent according to the number of functionality which is identical to the branch number.[16]

The critical condition is usually defined as the point at which the weak attractive enthalpic interaction effect is exactly compensated by the entropic exclusion effect for a linear homopolymer, and the polymer species elutes near the elution time of the injection solvent, independent of its molecular weight.[4,6,17] LCCC has been successfully employed for the characterization of a variety of complex polymer systems such as functionality analysis,[18] polymer blends,[19] block copolymers,[20–22] stereoregularity analysis,[23] cyclic polymers,[24] etc. The LCCC retention of branched polymers has been also examined theoretically by several authors.[15,25–27] In the theoretical works, an ideal chain model was employed to calculate the partition coefficient of branched polymers in a pore. Theoretical calculations showed that if star-shaped polymers are chemically the

* Corresponding authors. T.C.: Tel +82-54-279-2109, Fax +82-54-279-3399, e-mail tc@postech.ac.kr. Y.W.: Tel +1-901-678-2629, Fax +1-901-678-3447, e-mail ywang@memphis.edu.

10.1021/ma702377f CCC: $40.75
Published on Web 04/15/2008

Table 1. Molecular Characteristics of Star-Shaped PS Samples Determined by SEC with Light Scattering Detection

sample code	arm M_w (M_w/M_n)	star[a] M_w (M_w/M_n)
BS2.5-8.8	2 400 (1.06)	8 800 (1.81)
BS10-148	10 200 (1.02)	148 000 (1.7)
BS26-174	26 700 (1.01)	174 000 (2.18)

[a] As-prepared star-shaped PS sample after the linking reaction with DVB.

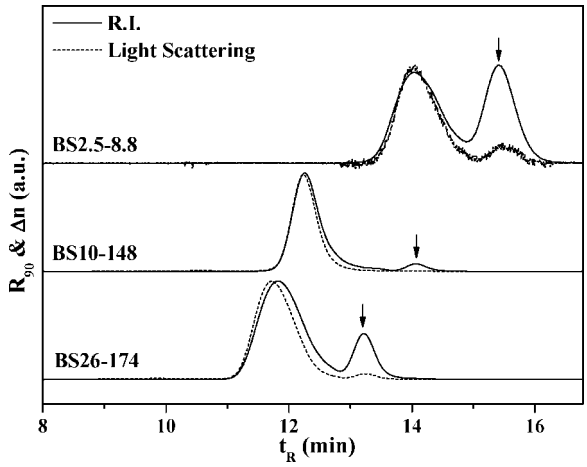

Figure 1. SEC chromatograms of three branched PS samples recorded with a refractive index detector (solid line) and a light scattering detector (dotted line). Separation conditions: two mixed bed columns (Polymer Laboratory, PL mixed C, 300 × 8 mm); THF eluent at a column temperature of 40 °C.

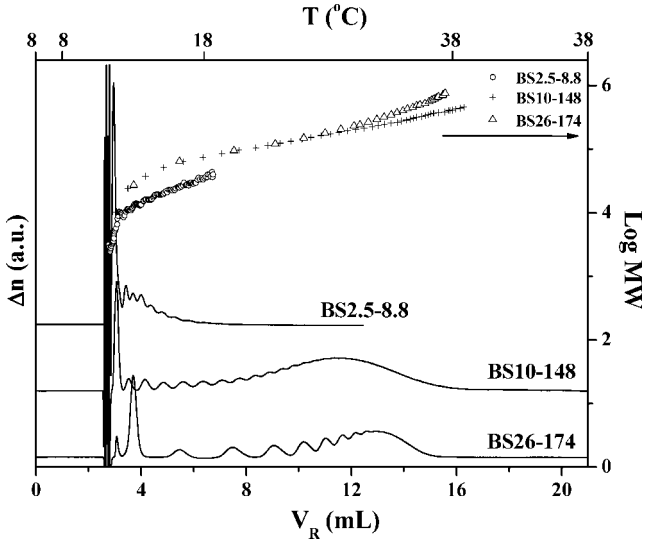

Figure 2. RP-TGIC separation of branched PS. The molecular weights obtained by light scattering detection are shown in the plot. The temperature program is shown in the top abscissa. Column: Nucleosil C18, 500 Å pore, 7 μm particle, 250 × 4.6 mm i.d. Eluent: CH_2Cl_2/CH_3CN (57/43, v/v) at a flow rate of 0.5 mL/min. Temperature program: 8 °C during the first 2 min, linear increase to 18 °C for 12 min, linear increase to 38 °C for 18 min, and kept at 38 °C for the next 8 min.

same and are at the critical condition, the partition coefficient of the star-shaped polymers is independent of chain architecture. Therefore, star-shaped polymers should coelute with the linear homopolymers at the critical condition according to theoretical expectation based on the ideal chain model.

However, this conclusion may need to be re-examined with a more appropriate model as the ideal chain model ignores the excluded volume interaction which may be present in real polymer systems. The previous simulation studies of Wang and

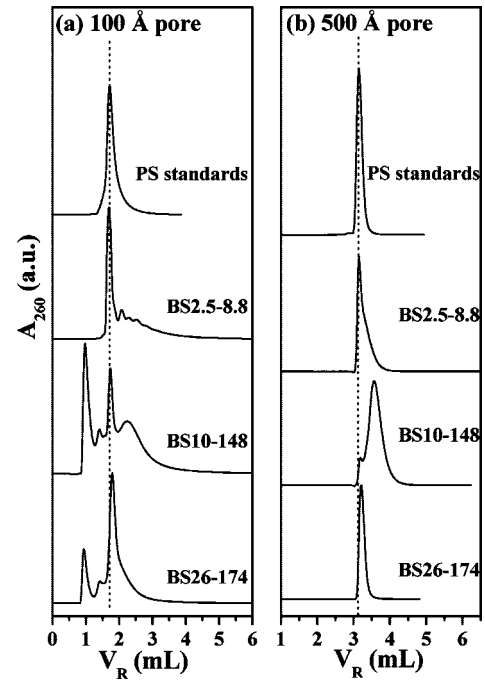

Figure 3. LCCC chromatograms of 5 PS standard samples (M_w: 7000, 30 900, 113 000, 200 000, and 384 000) and three star-shaped PS at the critical condition of PS. (a) Column: Kromasil C18, 100 Å pore, 5 μm particle, 150 × 4.6 mm. Column temperature: 33.3 °C. Eluent: CH_2Cl_2/CH_3CN (57/43, v/v) at a flow rate of 0.5 mL/min. (b) Column: Nucleosil C18, 500 Å pore, 7 μm particle, 250 × 4.6 mm i.d. Column temperature: 30.4 °C. Eluent: CH_2Cl_2/CH_3CN (57/43, v/v) at a flow rate of 0.5 mL/min.

co-workers have shown that the excluded volume has a nontrivial effect on LCCC retention behavior of linear polymers.[28,29] In addition, for star-shaped polymers with a higher number of branches, the core region is crowded with segments. When such stars are transferred into a pore, the confinement free energy cost will be higher than that for the linear polymers when the pore size is smaller than that of a polymer molecule. Therefore, the excluded volume interaction ignored in most theories could have a profound effect on the retention of stars in LCCC. In fact, an earlier Monte Carlo simulation of chains with excluded volume interactions indicated that the compensation of entropic loss and enthalpic adsorption in a slitlike pore depends on chain architecture.[30] It can be inferred from the reported simulation data that the retention of branched polymers differs from the linear polymers and depends on pore size and chain architecture.

In this study, we investigated the LCCC retention of star-shaped polymers at the critical condition defined by the coelution of linear polymers in two different pore size columns for a set of star-shaped polymers having different number and length of branches. The experimental results are then compared with Monte Carlo simulation results to elucidate the retention mechanism of branched polymers at the critical condition. The branched polymers are seen to exhibit a complex LCCC retention behavior, which can be explained by Monte Carlo simulation results that take into account both chain-end effects and the excluded volume interaction.

Experimental Section

Materials. The star-shaped PS samples were prepared by anionic polymerization of styrene and subsequent linking of the polystyryl anions with divinylbenzene. Details of the polymerization procedure were reported previously.[31] Three star polystyrene samples in the molar mass range of 2−400 kg/mol were used as listed in Table 1. In the sample code BS*X*-*Y*, *X* and *Y* stand for the weight average

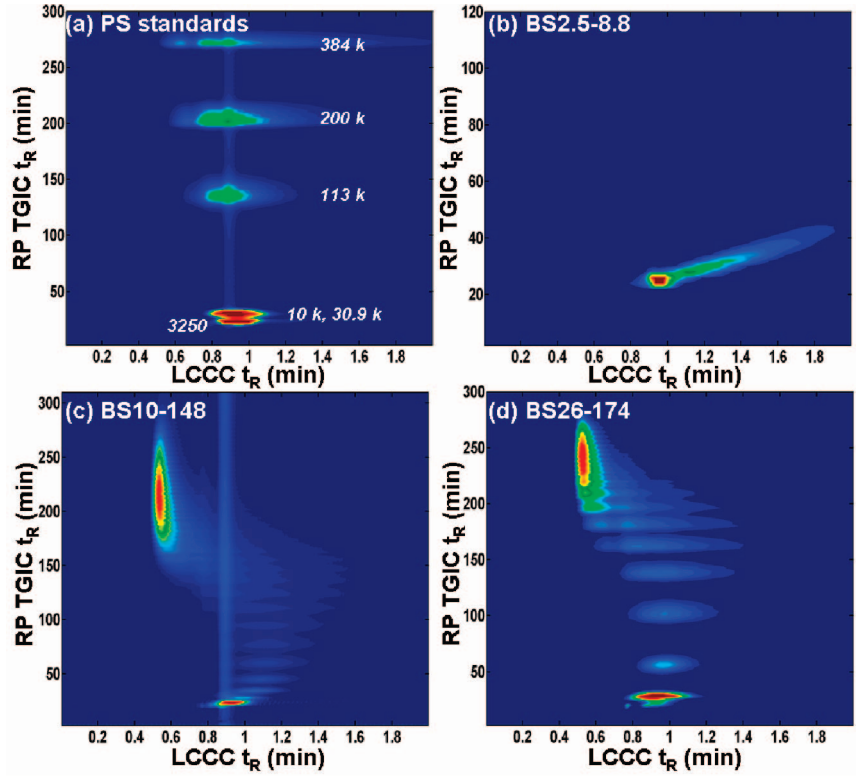

Figure 4. Contour plots of RP-TGIC × LCCC 2D-LC chromatograms of PS standards and star-shaped PS. (a) PS standards (MW: 3250, 10 000, 30 900, 113 000, 200 000, and 384 000), (b) BS2.5-8.8, (c) BS10-148, and (d) BS26-174. For RP-TGIC, column: Nucleosil C18, 100 Å pore, 7 μm particle, 250 × 2.1 mm i.d; eluent: CH_2Cl_2/CH_3CN (57/43, v/v) at a flow rate of 0.05 mL/min. For LCCC, column: Kromasil C18, 100 Å pore, 5 μm particle, 150 × 4.6 mm i.d.; column temperature: 28.1 °C; eluent: CH_2Cl_2/CH_3CN (57/43, v/v) at a flow rate of 1.9 mL/min.

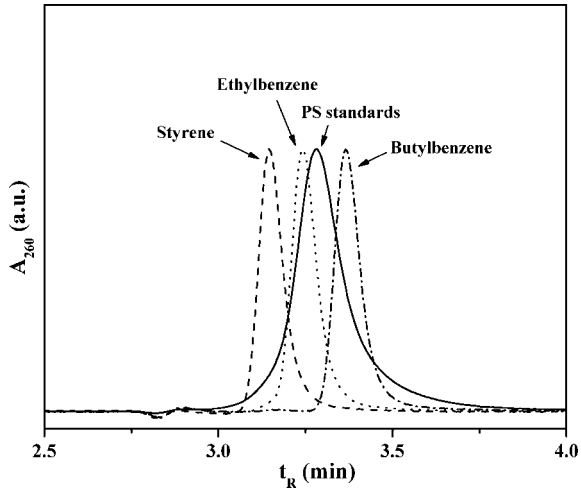

Figure 5. Chromatograms of styrene, ethylbenzene, and butylbenzene at the LCCC condition of PS (PS M_w: 1080, 2000, 10 000, and 30 900). Column: Kromasil C18, 100 Å pore, 5 μm particle, 150 × 4.6 mm i.d. Column temperature: 28.4 °C. Eluent: CH_2Cl_2/CH_3CN (57/43, v/v) at a flow rate of 0.5 mL/min.

MW of the branch and the star-shaped PS, respectively.

SEC Analysis. For the SEC analysis, two mixed-bed columns (Polymer Laboratories, PLgel Mixed-C, 300 × 7.5 mm) were used at a column temperature of 40 °C. SEC chromatograms were recorded with a light scattering/refractive index detector (Viscotek TDA 300) using THF (Samchun, HPLC grade) as the eluent at a flow rate of 0.8 mL/min. The dn/dc value of 0.185 was used. Polymer samples for the SEC analysis were dissolved in THF at a concentration of ~1.0 mg/mL, and the injection volume was 100 μL.

RP-TGIC and LCCC Analysis. For the reversed phase (RP)-TGIC separation, a C18 bonded silica column (Nucleosil C18, 7 μm, 500 Å, 250 × 4.6 mm) was used. The mobile phase was a CH_2Cl_2/CH_3CN mixture (57/43, v/v, Samchun, HPLC grade) delivered by a Bischoff HPLC compact pump at a flow rate of 0.5 mL/min. The temperature of the separation column was controlled by circulating fluid from a programmable bath/circulator (Thermo-Haake, C25P) through a homemade column jacket. The same chromatography system was used for the LCCC separation except for the separation columns. Two different pore size columns were used to study the pore size dependence: a C18 bonded silica column (Nucleosil C18, 7 μm, 500 Å, 250 × 4.6 mm) and a C18 bonded silica column (Kromasil C18, 5 μm, 100 Å, 150 × 4.6 mm). The injection samples were prepared by dissolving the polymer samples in the eluent. RP-TGIC chromatograms were recorded with a light scattering/refractive index detector (Viscotek TDA 300) to estimate the number of branches from the MW of the elution peak. LCCC chromatograms were recorded with a UV absorption detector (Thermo, UV 2000) operating at a wavelength of 260 nm.

RP-TGIC × LCCC 2D-LC Analysis. For the RP-TGIC × LCCC 2D-LC analyses, the same conditions as in the 1D-LC analysis were used except for the column and the flow rate. A C18 bonded silica column (Nucleosil C18, 7 μm, 500 Å, 250 × 2.1 mm) and a C18 bonded silica column (Nucleosil C18, 7 μm, 500 Å, 150 × 4.6 mm or Kromasil C18, 5 μm, 100 Å, 150 × 4.6 mm) were used for the 1st-D RP-TGIC and for the 2nd-D LCCC separations, respectively. The flow rate of the 1st-D RP-TGIC was set low at 0.05 mL/min to synchronize with the 2nd-D LCCC separation operated at a flow rate of 1.9 mL/min. The details of the comprehensive 2D-LC instrument were reported in previous reports.[16,32]

Monte Carlo Simulation. Lattice-based Monte Carlo simulations were carried out using two different chain models: (i) chains with no excluded volume interactions (random walks, RW) and (ii) chains with excluded volume interaction (self-avoiding walks, SAW). The simulation using the first model, RW, is expected to reproduce the previous theoretical prediction.[15,26,27] The second model, SAW, however is more realistic, and the results can be

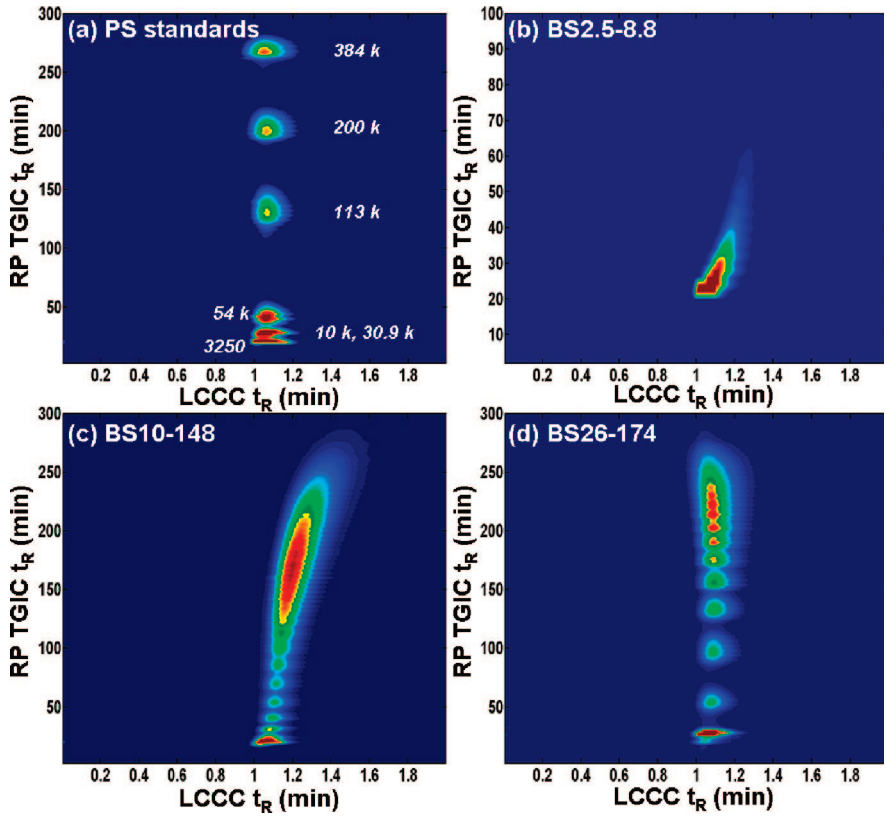

Figure 6. Contour plots of RP-TGIC × LCCC 2D-LC chromatograms of PS standards and branched PS: (a) PS standards (MW: 3250, 10 000, 30 900, 54 000, 113 000, 200 000, and 384 000), (b) BS2.5-8.8, (c) BS10-148, and (d) BS26-174. For RP-TGIC column: Nucleosil C18, 500 Å pore, 7 μm particle, 250 × 2.1 mm i.d. Eluent: CH_2Cl_2/CH_3CN (57/43, v/v) at a flow rate of 0.05 mL/min. For LCCC column: Nucleosil C18, 500 Å pore, 7 μm particle, 150 × 4.6 mm i.d. Column temperature: 33.5 °C. Eluent: CH_2Cl_2/CH_3CN (57/43, v/v) at a flow rate of 1.9 mL/min.

compared with experimental data. The lattice used is a simple cubic lattice with a coordination number $z = 6$ and $z = 26$ for the RW and the SAW models, respectively. On the $z = 6$ simple cubic lattice, the bond connecting the monomers assumes one of six orientations, (0, 0, ±1), and the associated permutations. On the $z = 26$ simple cubic lattice, the bond connecting the monomers assumes one of 26 orientations, (0, 0, ±1), (0, ±1, ±1), (±1, ±1, ±1), and the associated permutations. Both lattice models yield similar results for linear polymers, but the number of arms in a star cannot exceed the coordination number. Therefore, $z = 26$ simple cubic lattice was used for star polymers.

Since the critical condition point is model-dependent, the critical condition for each specific chain model was first determined. In a slitlike pore, the critical condition point was independent of pore size. The method to determine the critical condition point in simulation can be found in an earlier report.[29] In each set of simulations, the length of linear polymer chains N, measured by the total number of beads on the chain, is varied from 25 to 400. The stars contained different number of arms with fixed arm length of N_a. The arms are joined to a central bead. Hence, the total number of beads of a star $N_{total} = fN_a + 1$, where f is the number of arms ($f \leq z$). Each bead interacts with the surface sites in a slit pore via an attractive interaction energy ϵ, reduced by the Boltzman factor, k_BT, whenever the surface site is a nearest neighbor to the bead. The interaction of end beads of stars with the surface may differ from that of the inner beads. In the case of $z = 6$ simple cubic lattice, a bead sitting above the surface can only make one surface contact. In the case of $z = 26$ simple cubic lattice, a bead sitting above a surface make five surface contacts, and all five contacts are assumed to have the same pairwise interaction energy ϵ_a. As a result, the determined critical condition ϵ_a for SAW chains in $z = 26$ simple cubic lattice is seen to be smaller than the critical condition for SAW chain in the $z = 6$ simple cubic lattice. The partition coefficient K is determined via $-RT \ln K = \Delta\mu°$, where $\Delta\mu°$ is the standard chemical potential difference of a chain inside the pore from that in the bulk solution. The biased chain insertion method was used to determine the chemical potential. More details on the biased chain insertion method can be found in earlier reports.[28,29,33] Over 5−10 million copies of chain conformations were typically sampled.

Results and Discussion

SEC Separation of Branched Polymers. The PS samples prepared by linking polystyryl anions with divinylbenzene yields a set of star-shaped polymers with different number of narrowly dispersed arm length. Figure 1 displays the SEC chromatograms of the three branched PS. The solid line and dotted line are the chromatograms recorded by a refractive index detector and a light scattering detector, respectively. All the samples contain precursor PS resolved as a separate peak (marked with an arrow), but the differently branched species are not resolved at all. The characterization results of star PS are listed in Table 1.

TGIC Separation of Branched Polymers. TGIC separations were carried out under weakly adsorbing conditions near the critical condition. The interaction between the solute and the stationary phase is controlled by varying the column temperature during the elution.[34] The TGIC retention is less sensitive to the chain architecture than SEC and shows much higher resolution than SEC in separating polymers according to MW.[35] Figure 2 displays a RP-TGIC chromatogram of branched PS recorded by a refractive detector and MW determined by light scattering detection. The first peak eluting at $V_R \approx 3$ mL is the injection solvent peak, and a series of the following peaks represent star-shaped PS with increasing number of arms. These peaks were not resolved in SEC separation, which shows higher resolution of IC than SEC. The number of branches corresponding to each peak can be determined easily

by measuring the MW of each peak by light scattering detection, which differs by an integral multiple of the arm MW.[7]

As the number of arms increases, the elution peaks start to overlap. This is mainly due to the overlap of the finite MW distribution of the branched species even though the PS samples were prepared by anionic polymerization to have a very narrow MW distribution close to the Poisson distribution.[12,36] The MW determined by light scattering shows an interesting behavior: the MW of BS2.5-8.8 departs significantly from the other two samples, and BS10-148 and BS26-174 also depart from each other as the branch number increases. Such a clear deviation has not been observed in previous works on branched polymers with fewer numbers of longer branches.[7,8,13] Therefore, we suspect that this behavior is due to increased chain end (in this case the initiator moiety) effect on the retention of stars with a large number of relatively short branches.[11] It can be conjectured from these data that the chain ends are more adsorptive than the repeating units of PS in the TGIC separation condition, which also coincides with the retention trend observed in the LCCC condition presented shortly after.

1D-LCCC Separation of Branched Polymers. Figure 3 displays the chromatograms of linear PS standards and three branched PS samples at the critical condition of two different pore size columns, (a) 100 Å and (b) 500 Å. At a fixed mobile phase composition (CH_2Cl_2/CH_3CN = 57/43, v/v), the column temperature was adjusted to find the coelution point of several linear PS standards. Five different MW PS standard samples (M_w: 7000, 30 900, 113 000, 200 000, and 384 000) were used. The critical condition was found as 33.3 °C for the 100 Å pore column and 30.4 °C for the 500 Å pore column. The coelution peak of the linear standards is sharp for the 500 Å pore column while it is broad for the 100 Å pore column. It was reported previously that the elution peak of high-MW polymer is broadened near the critical condition, and the effect is larger for small pore size column.[24] The dotted vertical line in Figure 3 marks the coelution volume of the linear PS samples for visual aid. If the LCCC retention of branched polymer is identical to the linear polymers, the branched PS should elute at the coelution volume of the linear standards. However, the LCCC chromatograms are far from the expectation. For the case of the 100 Å pore column (a), the chromatograms of the branched PS have a complicated shape. BS2.5-8.8 elutes after the coelution volume of the linear PS while BS10-148 and BS26-174 elute at both smaller and larger retention volumes than the coelution volume of linear polymers. The LCCC chromatograms obtained with the 500 Å pore column (b) show less distinct features than that of 100 Å pore column, but the branched polymers elute later than the linear PS. It is clear that the retention of the branched PS is different from that of linear PS at the critical condition of linear polymers.

RP-TGIC × LCCC 2D-LC Separation of Branched Polymers. To scrutinize the LCCC retention behaviors of the branched PS, we carried out 2D-LC separation by combining RP-TGIC and LCCC as the 1st-D and the 2nd-D LC separation, respectively. From the 2D-LC chromatogram, we can easily see how the LCCC retention is affected by the number of branches since the branched PS is separated according to the branch number through the 1st-D RP-TGIC separation. Figure 4 shows the 2D-LC chromatograms of the linear PS samples and three branched PS with the 100 Å pore size column. Figure 4a shows the coelution behavior of the six different linear PS samples. The faint vertical line appearing at $t_R \approx 0.9$ min is the injection solvent peak for the second-D LCCC separation. The linear PS samples apparently coelute near the injection solvent peak position, but the elution peaks show significant broadening. This is a typical phenomenon at the LCCC condition if a small pore size column is used.[24]

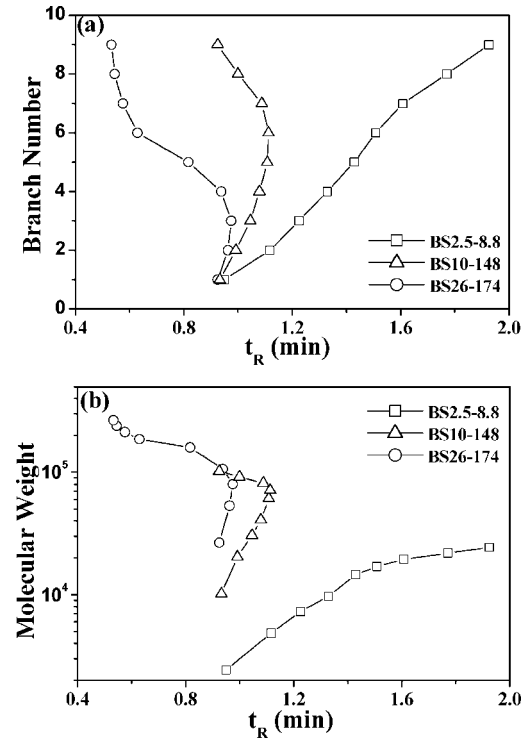

Figure 7. (a) Branch number and (b) molecular weight vs LCCC retention time for three branched PS for 100 Å pore column. These curves were constructed from the 2D-LC chromatograms shown in Figure 4.

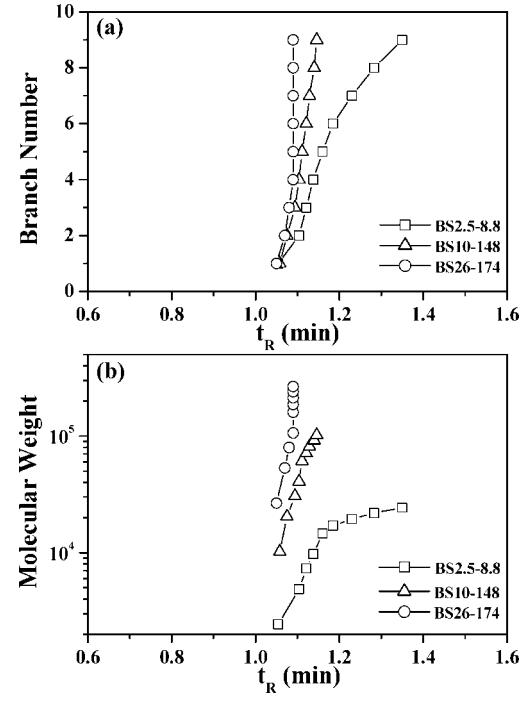

Figure 8. (a) Branch number and (b) molecular weight vs LCCC retention time for three branched PS for a 500 Å pore column. These curves were constructed from the 2D-LC chromatograms shown in Figure 6.

BS2.5-8.8 elutes later than the coelution point of linear PS, and the retention time increases as the branch number increases (Figure 4b). This explains why the 1D-LCCC chromatogram shown in Figure 3 has a long tail. The data also indicate that the interaction of the BS2.5-8.8 becomes more adsorptive to the stationary phase with an increase of the branch number. As alluded to in the RP-TGIC retention behavior in Figure 2, the

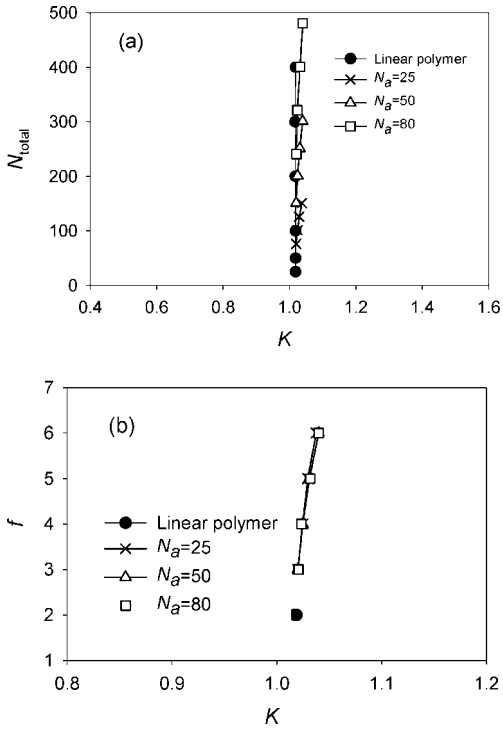

Figure 9. Comparison of partition coefficients of stars with linear polymers modeled as random walks on simple cubic lattice with coordination number $z = 6$. All beads interact with the surface with the same interaction energy $\epsilon_a = -0.182\,32$, which is the critical condition for the linear polymers. N_a is the arm length of the stars and in each series the number of arms $f = 3$, 4, 5, and 6. (a) Dependence of K on the total number of segments. (b) Dependence of K on the number of end monomers in the stars. The slit width $D = 19$.

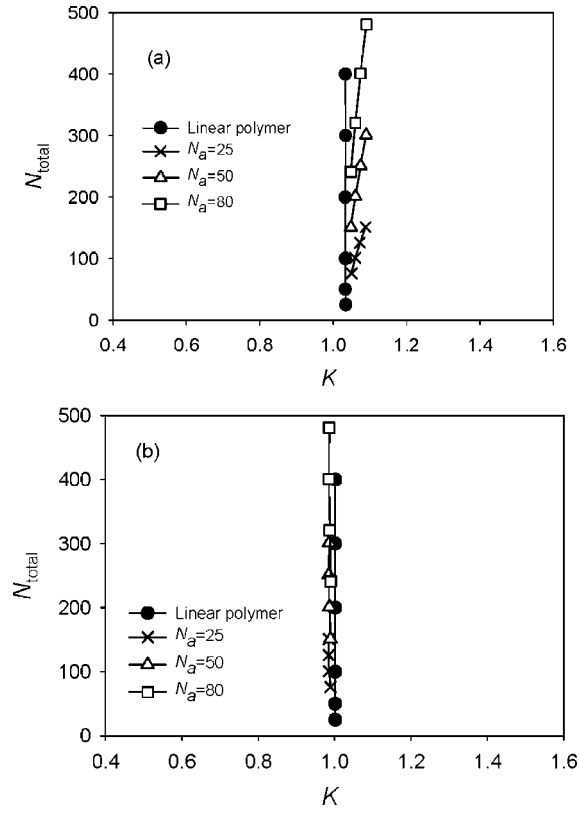

Figure 10. Comparison of the partition coefficients of stars with linear polymers modeled as random walks in simple cubic lattice with $z = 6$. All middle beads interact with the surface at $\epsilon_a = -0.182\,32$, while the end beads interact with the surface differently. (a) Surface interaction energy of end beads $\epsilon^{end} = -0.25$. (b) Surface interaction energy of end beads $\epsilon^{end} = -0.10$. The slit width $D = 19$.

end functionality is suspected to be the origin of this phenomenon, as each branch of the star-shaped PS has a butyl end group from the initiator of anionic polymerization. To further verify the functionality effect, the retention of styrene (as the model for an unreacted vinyl group of divinylbenzene in the core), ethylbenzene (as the model for a PS segment), and *n*-butylbenzene (as the model for a butyl chain end) was examined at the LCCC condition of linear PS, and the results are displayed in Figure 5. Butylbenzene is retained longer than other substance while styrene shows the shortest retention time, clearly indicating that the butyl chain ends are most adsorptive at this separation condition and that the possible residual double bonds in the core is less absorptive than the repeating unit of PS.

While the extent of the deviation from linear PS retention is reduced with the increase of branch MW, a similar trend of increasing retention with branch number is observed (Figure 4c,d). As the number of branches increases further in Figure 4c,d, the elution peaks make a turn to lower retention times and cross the coelution point of the linear PS to elute before the injection solvent peak (SEC regime). Finally, the heavily branched polymers elute unresolved at $t_R \sim 0.5$ min, which is the total exclusion point of the column. The heavily branched PS with long branches (>10 000) seem to be excluded from the pore at the LCCC, illustrating why the 1D-LCCC chromatograms of BS10-148 and BS26-174 in Figure 3a show sharp peaks at $V_R \sim 1$ mL.

The LCCC retention behavior strongly depends on the pore size. Figure 6a shows the LCCC condition for a 500 Å pore column with linear PS standards. Compared with Figure 4a for the 100 Å pore column, the elution peaks with the larger pores size column are narrower. The LCCC retention behavior of the branched PS shows similar trends with both pore sizes, but the retention in the 500 Å column changes with the branch number to a far lesser extent. For low MW branches (b: BS2.5-8.8), the LCCC retention increases with number of branches, which results in a moderate tailing in the 1D-LCCC chromatogram in Figure 3b. For the BS10-148 (c), the LCCC retention increases with the number of arms slightly and does not show a turnover behavior. As the branch MW increases to 26 000 (d: BS26-174), the LCCC retention appears nearly MW independent. These 2D-LC chromatograms are consistent with the 1D-LCCC chromatogram shown in Figure 3b. Although the MW independent elution of branched PS is not realized with the 500 Å pore column, the deviation from the coelution behavior is far less severe than in 100 Å pore column, and no turnover to the SEC regime is observed in the 500 Å column.

Although the 2D-LC chromatograms show how the LCCC retention time changes with MW of the star-shaped PS, the MW dependence of the RP-TGIC retention is different for each star-shaped PS as shown in Figure 2. To compare them in the same scale, the 2D-LC chromatograms are replotted in Figures 7 and 8 for 100 and 500 Å pore size columns, respectively. They show the plots of branch number (a) and log MW (b) vs retention time for three branched PS. In Figure 7, for the 100 Å pore column, as the branch number increases, the retention increases at first and makes a turn to decrease. The branch number at the turning point decreases as the branch MW increases: BS2.5-8.8 does not make a turn, BS10-148 makes a turn at the branch number around 6, and BS26-174 makes a turn at 3. On the other hand, for the 500 Å pore column (Figure 8), as the branch number increases, the retention increases but to a much lesser extent than the case of 100 Å pore column. Furthermore, the turnover behavior is not clearly seen. Only BS26-174 appears to start the turn at the high branch number but it is rather ambiguous.

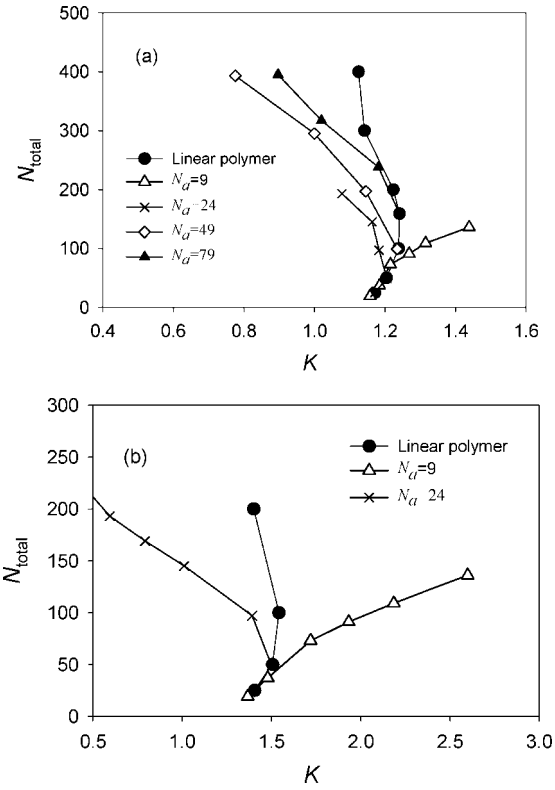

Figure 11. Partition coefficient of stars and linear polymers modeled as SAW in simple cubic lattice with a coordination number z = 26 at the critical condition, $\epsilon_a = -0.06$. All beads interact with the surface with $\epsilon = \epsilon_a$. (a) Partition into a slit pore with width $D = 19$. (b) Partition into a slit pore with width $D = 9$.

Combining the observations made in the 2D-LC analysis, we would like to propose that the initial increase of retention volume with branch number is due to the increase of the end functionality, which is more adsorptive to the stationary phase than the polymer chain segments. BS2.5-8.8 has a size smaller than the pore size of the columns, and all chain ends can interact with the stationary phase efficiently. As the arm length increases, the size of stars becomes comparable to the pore size and starts to be excluded from the pores. The exclusion effect must be larger for longer armed and more highly branched stars at smaller pore size column. Therefore, the retention volume of BS10-148 and BS26-174 starts to decreases as the branch number increases, and the exclusion effect shows up at lower branch number for longer arm stars. In principle, the exclusion effect is supposed to be compensated by the attractive interaction at the critical point, but the exclusion effect of branched polymers seems to be stronger than the linear polymers. Next, we would like to validate the proposed explanation for the complex LCCC retention behavior by comparing the experimental observation with Monte Carlo simulations.

Monte Carlo Simulation of LCCC Retention of Branched Polymers. We first present results when chains are modeled as reversible random walks (ideal chains) on a simple cubic lattice with a coordination number $z = 6$. The critical condition is known theoretically as $\epsilon_a = \ln(1 - \lambda) = -0.182\,32$, where $\lambda = 1/6$.[37] Figure 9a presents the dependence of the partition coefficient K on the total number of beads N_{total} of stars and linear polymers at the critical condition. All beads interact with the surface with the same energy $\epsilon_a = -0.182\,32$. The partition coefficients K for stars are slightly larger than that for linear polymers, but they are very close to each other. In Figure 9b, the y-axis is changed to the number of end beads. The partition coefficients of the stars are now more clearly seen to be different

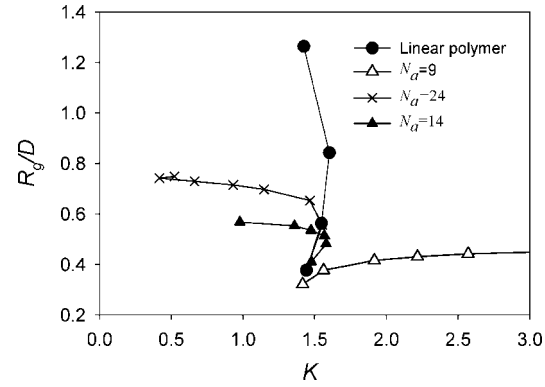

Figure 12. Partition coefficient of stars and linear polymers modeled as SAW in simple cubic lattice with a coordination number z = 26 at the critical condition, $\epsilon_a = -0.06$. The surface interaction energy of end beads $\epsilon^{end} = -0.065$ while surface interaction energy of the rest of beads is at $\epsilon = \epsilon_a = -0.06$. The slit width $D = 9$. The y-axis is R_g/D, where R_g is the radius of gyration of the stars. The number of arms in stars with $N_a = 9$ are $f = 2$, 4, 6, 10, and 12. The number of arms in stars with $N_a = 24$ are $f = 2$, 4, 6, 8, 10, and 12. The number of arms in stars with $N_a = 14$ are $f = 1$, 2, 4, 6, 7, 8, 9, and 10 (data points for $f = 1$ and 2 are covered up by data points of linear homopolymers).

from the linear polymers, and the difference is dependent on the number of branches, not the branch length. The results are similar to those obtained when the end beads are set to be slightly more adsorptive than the inner beads, which will be presented shortly in Figure 10. It seems that at the critical condition the enthalpy gain and the entropy loss in the random walk models are perfectly balanced for the middle beads, but not for the end beads. The end beads, having more coordination numbers to interact with the surface, are slightly more adsorptive. So as the number of branches increases, the stars are slightly more retained even when the stars are modeled as random walks.

We then explored the situation when the chain ends interact with the surface differently from the rest of beads. Figure 10 presented the two scenarios: (a) when the ends are more attractive than the rest of beads and (b) when ends are less attractive than the rest of beads. When the chain ends are more attractive to the surface, the stars are more retained in the pore. Moreover, the partition coefficient of the stars is proportional to the number of arms and is independent of arm lengths. This result is in good agreement with the previous report of Radke et al. with end-functional star-shaped poly(lactide)s.[15] On the other hand, when the ends are less attractive to the surfaces, both the linear polymers and the stars had a slightly smaller K. The partition coefficients of the stars are slightly smaller than that of linear polymers, but no crossover to the exclusion regime is seen. Therefore, the ideal chain model cannot explain the observed elution behavior of the star-shaped PS at the critical condition of linear polymers.

Now we present results when stars and linear polymers are modeled as self-avoiding walks (SAW) in a simple cubic lattice with a coordination number $z = 26$. The critical condition for this model was first determined to be at $\epsilon_a = -0.060$, following the method used earlier.[29] The elution behavior of stars and linear polymers in a slit pore at the critical condition are compared in Figure 11. For the SAW model, the partition coefficient K at the critical condition is not entirely independent of the chain length but has a slight curvature, which is more pronounced for smaller slit widths. The results for the SAW show an interesting phenomenon. The stars with short arms ($N_a = 9$) are more retained than the linear polymers. On the other hand, stars with longer arms ($N_a = 24$, 49, and 79) were less retained than linear polymers, and in some cases the stars are

in the exclusion regime (defined as $K \gtrsim 1$). This phenomenon is more evident in a smaller slit such as in $D = 9$, as shown in Figure 11b. If the slit width increases, all the lines tend to move closer to the line for linear polymers with smaller curvature. We further found that the stars are in the exclusion regime when its bulk radius of gyration R_g is about half of the slit width (an example of this is shown in Figure 12), i.e., when the stars feel the confinement imposed by the slit pore. Similar characteristics are observed from the results where the stars are modeled as SAW chains in simple cubic lattice with a coordination number $z = 6$ for the stars of $f \leq 6$.

The results about stars being excluded from the slit pore when its size becomes larger than the pore size are not too surprising. The core of stars with high number of arms is rather dense and is difficult to compress. Therefore, the gain of enthalpic interaction energy cannot offset the cost of confining the stars. Hence, stars may be excluded from the pore when their sizes are larger than the pore size. The result for stars with short arms being more retained than the linear polymers is of a little surprise. Our explanation is that for SAW at the critical condition the beads are slightly adsorptive, and the end beads are even more adsorptive than inner beads since the ends have more coordination numbers to interact with the surface. A star with many arms has more end beads interacting favorably with the surfaces than a linear polymer could have. Therefore, the star is more retained than the linear polymers.

The simulation results so far presented however do not exhibit phenomena where stars with a few arms are first retained more in the slit but become excluded as the number of arms increases. We have observed only scenarios where either the stars are more retained or are less retained than the linear polymers. Figure 12 presents the results when the end beads interact with the surface with $\epsilon^{end} = -0.065$, slightly more adsorptive than the rest of beads at the critical condition. The stars with arm length $N_a = 14$ now demonstrate the crossover from being slightly more retained than the linear polymer to being less retained than the linear polymer. Note the interaction energy of the end beads differs from the rest of beads by only 10%. We have not explored other interaction energies of the end beads but suspect that if the end beads differ more from the rest of beads, then stars with other arm lengths such as $N_a = 24$ will also exhibit such crossover. The general behavior is very similar to what was observed experimentally as shown in Figures 7 and 8. Although the consistency with the simulated data may not constitute proof, it is quite convincing that the end group effect and the excluded volume effect both need to be considered to interpret the complex LCCC retention behavior of the star-shaped PS observed in experiments.

Summary

The retention of star-shaped branched polystyrenes at the critical condition point defined by the coelution of its corresponding linear polymers has been investigated with RP-TGIC × LCCC 2D-LC separation and lattice Monte Carlo simulation. The branched polymers did not coelute with the linear polymers but instead eluted either before or after the coelution point depending on the branch numbers and the arm length. The dependence of retention on the branch numbers and the arm length is best delineated with the 2D-LC separation: (1) The LCCC retention time increases first as the branch number increases. (2) Then the elution time decreases as the number of branches further increases. The turnover point in terms of the branch number is lower for the star PS with higher MW arms. (3) As the number of branches further increases, it crosses over the coelution point and the heavily branched PS (thus very high MW) elute in the SEC regime eventually reaching the total exclusion limit of the column. (4) The general trend is more clearly observed for 100 Å pore column than 500 Å pore column.

The experimental results could be well explained by considering two factors: the chain end effects and the excluded volume interaction. The first factor has been considered earlier in the study by Radke et al.[15] When the chain ends are more adsorptive in the columns, the stars are found to be more retained than the linear polymers. However, the current study also observes instances where highly branched stars are eluted in the exclusion regime. This later phenomenon is attributed to the excluded volume interaction ignored in most theoretical discussion.[15,25–27] Monte Carlo simulation results with a chain model that has both excluded volume interaction and more adsorptive chain ends are found to best reproduce experimental data. Therefore, the excluded volume interaction and chain end effect seem to both play a significant role in differentiating the LCCC retention of star-shaped polymers from their linear counterparts.

Acknowledgment. T.C. acknowledges the support from KOSEF through the Center for Integrated Molecular Systems and the National Research Laboratory Program. Y.W. acknowledges the financial support from ACS/PRF under Grant 46933-AC7 and National Science Foundation under Grant CHE-0724117 (cofunded by MPS/CHE and OISE).

References and Notes

(1) Mishra, M. K.; Kobayashi, S. *Star and Hyperbranched Polymers*; Marcel Dekker: New York, 1999; p 350.
(2) Inoue, K. *Prog. Polym. Sci.* **2000**, *25*, 453–571.
(3) Rudin, A. Measurement of Long-Chain Branch Frequency in Synthetic Polymers. In *Modern Methods of Polymer Characterization*; Barth, H. G., Mays, J. W., Eds.; Wiley: New York, 1991; pp 103−150.
(4) Pasch, H.; Trathnigg, B. *HPLC of Polymers*; Springer-Verlag: Berlin, 1997.
(5) Chang, T. *Adv. Polym. Sci.* **2003**, *163*, 1–60.
(6) Macko, T.; Hunkeler, D. *Adv. Polym. Sci.* **2003**, *163*, 61–136.
(7) Lee, H. C.; Chang, T.; Harville, S.; Mays, J. W. *Macromolecules* **1998**, *31*, 690–694.
(8) Lee, H. C.; Lee, W.; Chang, T.; Yoon, J. S.; Frater, D. J.; Mays, J. W. *Macromolecules* **1998**, *31*, 4114–4119.
(9) Perny, S.; Allgaier, J.; Cho, D.; Lee, W.; Chang, T. *Macromolecules* **2001**, *34*, 5408–5415.
(10) Cho, D.; Park, S.; Chang, T.; Avgeropoulos, A.; Hadjichristidis, N. *Eur. Polym. J.* **2003**, *39*, 2155–2160.
(11) Im, K.; Park, S.; Cho, D.; Chang, T.; Lee, K.; Choi, N. *Anal. Chem.* **2004**, *76*, 2638–2642.
(12) Ryu, J.; Im, K.; Yu, W. J.; Park, J.; Chang, T.; Lee, K.; Choi, N. *Macromolecules* **2004**, *37*, 8805–8807.
(13) Gerber, J.; Radke, W. *Polymer* **2005**, *46*, 9224–9229.
(14) Biela, T.; Duda, A.; Pasch, H.; Rode, K. *J. Polym. Sci., Part A: Polym. Chem.* **2005**, *43*, 6116–6133.
(15) Radke, W.; Rode, K.; Gorshkov, A. V.; Biela, T. *Polymer* **2005**, *46*, 5456–5465.
(16) Im, K.; Kim, Y.; Chang, T.; Lee, K.; Choi, N. *J. Chromatogr. A* **2006**, *1103*, 235–242.
(17) Belenkii, B. G.; Gankina, E. S.; Tennikov, M. B.; Vilenchik, L. Z. *Dokl. Akad. Nauk SSSR* **1976**, *231*, 1147.
(18) Entelis, S. G.; Evreinov, V. V.; Gorshkov, A. V. *Adv. Polym. Sci.* **1986**, *76*, 129–175.
(19) Pasch, H. *Polymer* **1993**, *34*, 4095–4099.
(20) Zimina, T. M.; Kever, J. J.; Melenevskaya, E. Y.; Fell, A. F. *J. Chromatogr.* **1992**, *593*, 233–241.
(21) Lee, H.; Lee, W.; Chang, T.; Choi, S.; Lee, D.; Ji, H.; Nonidez, W. K.; Mays, J. W. *Macromolecules* **1999**, *32*, 4143–4146.
(22) Lee, W.; Cho, D.; Chang, T.; Hanley, K. J.; Lodge, T. P. *Macromolecules* **2001**, *34*, 2353–2358.
(23) Berek, D.; Janco, M.; Hatada, K.; Kitayama, T.; Fujimoto, N. *Polym. J.* **1997**, *29*, 1029–1033.
(24) Lee, W.; Lee, H.; Lee, H. C.; Cho, D.; Chang, T.; Gorbunov, A. A.; Roovers, J. *Macromolecules* **2002,** *35*, 529–538.
(25) Dimarzio, E. A.; Guttman, C. M.; Mah, A. *Macromolecules* **1995**, *28*, 2930–2937.
(26) Kosmas, M.; Kokkinos, I.; Bokaris, E. P. *Macromolecules* **2001**, *34*, 75377543.

(27) Gorbunov, A. A.; Vakhrushev, A. V. *J. Chromatogr. A* **2005**, *1064*, 169–181.
(28) Gong, Y. C.; Wang, Y. M. *Macromolecules* **2002**, *35*, 7492–7498.
(29) Orelli, S.; Jiang, W. H.; Wang, Y. M. *Macromolecules* **2004**, *37*, 10073–10078.
(30) Chen, Z.; Escobedo, F. A. *Phys. Rev. E.* **2004**, *69*, 021802/1–021802/10.
(31) Lee, H.-J.; Lee, K.; Choi, N. *J. Polym. Sci., Part A: Polym. Chem.* **2005**, *43*, 870–878.
(32) Im, K.; Park, H.-W.; Kim, Y.; Chung, B.; Ree, M.; Chang, T. *Anal. Chem.* **2007**, *79*, 1067–1072.
(33) Jiang, W. H.; Khan, S.; Wang, Y. M. *Macromolecules* **2005**, *38*, 7514–7520.
(34) Ryu, J.; Chang, T. *Anal. Chem.* **2005**, *77*, 6347–6352.
(35) Chang, T. *J. Polym. Sci., Polym. Phys.* **2005**, *43*, 1591–1607.
(36) Lee, W.; Lee, H.; Cha, J.; Chang, T.; Hanley, K. J.; Lodge, T. P. *Macromolecules* **2000**, *33*, 5111–5115.
(37) Fleer, G. J.; Cohens Stuart, M. A.; Scheutjens, J. M. H. M.; Cosgrove, T.; Vincent, B. *Polymers at Interfaces*; Chapman & Hall: London, 1993.

MA702377F